Hindawi Publishing Corporation
EURASIP Journal on Wireless Communications and Networking
Volume 2007, Article ID 81864, 14 pages
doi:10.1155/2007/81864

Research Article

Wireless Sensor Networks: Performance Analysis in Indoor Scenarios

G. Ferrari, P. Medagliani, S. Di Piazza, and M. Martalò

Wireless Ad-Hoc and Sensor Networks (WASN) Laboratory, Department of Information Engineering, University of Parma, 43100 Parma, Italy

Received 1 July 2006; Revised 8 December 2006; Accepted 2 January 2007

Recommended by Marco Conti

We evaluate the performance of realistic wireless sensor networks in *indoor* scenarios. Most of the considered networks are formed by nodes using the Zigbee communication protocol. For comparison, we also analyze networks based on the proprietary standard Z-Wave. Two main groups of network scenarios are proposed: (i) scenarios with *direct transmissions* between the remote nodes and the network coordinator, and (ii) scenarios with *routers*, which relay the packets between the remote nodes and the coordinator. The sensor networks of interest are evaluated considering different performance metrics. In particular, we show how the *received signal strength indication* (RSSI) behaves in the considered scenarios. Then, the network behavior is characterized in terms of *end-to-end delay* and *throughput*. In order to confirm the experiments, analytical and simulation results are also derived.

1. INTRODUCTION

Sensor networks have been a fertile research area, during the last years [1], for military applications, for example, remote monitoring, surveillance of reserved areas, and so forth. In a war scenario, in fact, cables may be damaged either by bombs or by enemies, and therefore, wireless technologies have been exploited in order to make the networks more robust against communication problems. First examples of military wireless sensor networks were the *SOund SUrveillance System* (SOSUS) [2] and the *Airborne Warning And Control System* (AWACS) [3]. In the last years, an increasing number of civilian applications of wireless sensor networks have been developed [4], especially for environmental monitoring [5]. The increasing interest in wireless sensor networks is driven by the current technologies, which guarantee the availability of low power consumption and low-cost devices.

The most attractive standard for wireless sensor networks is the IEEE 802.15.4 standard [6], which provides low-rate and energy-efficient data transmissions. The corresponding network architecture can be considered as a good compromise between hierarchical networks (e.g., those based on the IEEE 802.11 standard [7]) and networks with lower power consumption (e.g., those based on the IEEE 802.15.1 standard [8]). All these systems operate in the 2.4 GHz band: a comparison and a study of coexistence among them and other wireless networks are presented in [9]. Other issues about wireless sensor networks have also been considered. Besides coexistence, in [10] the authors analyze the problem of time synchronization in wireless sensor networks and propose an optimized flooding protocol for master-slave scenarios. In particular, different functionalities for real-time support have been analyzed and proposed for the Zigbee stack. Moreover, in [11] the authors show an experimental evaluation of a wireless sensor network using the Zigbee standard. In [12], instead, the author proposes a complete analysis of the main design parameters of wireless sensor networks, such as the received signal strength indication (RSSI), throughput, and packet delivery ratio. Finally, in [13] the authors analyze the path capacity of an IEEE 802.15.4 network, through SenProbe, a new path capacity estimation tool specifically designed for carrier-sense multiple-access with collision avoidance (CSMA/CA)-based wireless ad hoc networks.

In this paper, we analyze the performance of realistic wireless sensor networks in various *indoor* scenarios. Similar to [11, 12], we use common performance indicators (such as RSSI, throughput, and delay) in order to characterize the network behavior. Unlike [11, 12], we use the wireless sensor networking technologies developed by microchip [14] (*open standard*, Zigbee) and Zensys [15] (*proprietary standard*,

Z-Wave [16]), respectively. We try to highlight similarities and differences between the considered technologies, referring also to other possible choices, such as those described in [11, 12]. Moreover, we show how different performance metrics, such as packet error rate (PER) and delay, strongly depend on the distribution of the sensors in the indoor environment. In particular, our results show that the network connectivity has a *bimodal behavior* [17].

In order to validate the experimental results, the performance of Zigbee networks is evaluated using Opnet network simulator [18], in a scenario where remote nodes communicate directly to the network coordinator. Finally, a simple asymptotic (for a large number of sensors) performance analysis is provided, confirming further the experimental results.

The rest of this paper is structured as follows. In Section 2, we describe the functionalities provided by Zigbee (Section 2.1) and Z-Wave (Section 2.2) networking technologies. In Section 3, the wireless sensor network scenarios of interest are described. In Section 4, the obtained results, in terms of the chosen performance indicators (i.e., RSSI, throughput, and delay) are presented. In Section 5, simulation results are shown and a simple analytical framework, valid in an *asymptotic* (for large numbers of sensors) regime, is derived. Finally, Section 6 concludes the paper.

2. PRELIMINARIES ON SENSOR NETWORKS

2.1. Zigbee networks

The increasing need for applications where nodes can send data without the constraints imposed by the presence of power and transmission cables have led to the creation of *low-rate wireless personal networks* (LR-WPANs). This is the case, for example, of remote monitoring of natural events, such as landslides, earthquakes, and so forth [5, 19]. One of the newest standards for wireless sensor networks, with significant power savings, has been called Zigbee [20]. More precisely, the Zigbee alliance provides instructions only for the upper layers (i.e., from the third to the seventh layer) of the ISO/OSI stack [21]. At the first layers levels of the ISO/OSI stack (physical, PHY, and medium access control, MAC), the Zigbee technology is based on the IEEE 802.15.4 standard and guarantees (theoretically) a transmission data rate equal to 250 kpbs in a wireless communication link. Three transmission bands are allowed by the Zigbee standard: (i) 2.4 GHz, (ii) 868 MHz, and (iii) 916 MHz. While the first transmission band is available worldwide, the second and third are available only in Europe and USA, respectively.

Three different kinds of nodes can be used in a wireless network, according to the Zigbee specifications: (i) a *router*, (ii) a *coordinator*, (iii) and an *end device*. The coordinator can create the network, exchange the parameters used by the other nodes to communicate (e.g., network ID, beginning of a transmitted frame, etc.), relay packets received from remote nodes towards the correct destination, and collect data from the sensors. Only a single coordinator can be used in a network. A router, instead, relays the received packets and the control messages (in order to increase the network diameter), manages the routing tables and, if required, can also collect data from a sensor. The main difference between a coordinator and a router is that the former can create the network, while the latter cannot. Both these types of nodes are referred to as *full function devices* (FFDs): they can develop all the functions required by the Zigbee standard in order to set up and manage the communications. On the other hand, end devices, also referred to as *reduced function devices* (RFDs), can act only as remote peripherals, which collect values from sensors and send them to the coordinator or other remote nodes. However, RFDs are not involved in network management, and therefore, cannot send or relay control messages. According to the Zigbee standard, three different kinds of network topologies are possible, as shown in Figure 1: (i) *star*, (ii) *cluster-tree*, and (iii) *mesh*.

(i) In a *star* network, there are a coordinator and one or many RFDs (end nodes) or FFDs (routers) which send messages directly to the coordinator (up to 65536 RFDs or FFDs).

(ii) In a *cluster-tree* topology, instead, there are a coordinator which acts as a root and either RFDs or routers connected to it, in order to increase the network dimension. The RFDs can only be the leaves of the tree, whereas the routers can also act as branches. In a cluster-tree topology, a beacon structure can be employed in order to obtain an improved battery conservation.

(iii) In a *mesh* network, any source node can talk directly to any destination. The routers and the coordinator, in fact, are connected to each other, within their transmission ranges, in order to ease packet routing. The radio receivers at the coordinator and routers must be "on" all the time.

In a wireless mesh sensor network, a routing technique must be used. The Zigbee standard employs a simplified version of the *ad hoc on-demand distance vector* (AODV) routing protocol [22]. The AODV protocol is a reactive protocol in which the route is formed upon a route request generated by a (source) node. Through an exchange of messages between source and destination, the route can be reserved by intermediate nodes just updating their routing tables, so that communications can be guaranteed.

Since the main goal of a Zigbee network is data transmission under the constraint of maximum power saving, a *beacon* frame structure can be employed, as shown in Figure 2 [23]. The beacon frame is divided into two main periods, referred to as *active* and *inactive*, respectively. While in the latter period all nodes go to the sleeping state to preserve their battery energy,[1] in the former period all nodes can transmit their data packets. In order to prevent collisions, two different access techniques can be employed. In the *contention access period* (CAP), every node can transmit according to the

[1] In the sleeping state, nodes can reach energy savings which are three orders of magnitude higher than those in the active phase [24].

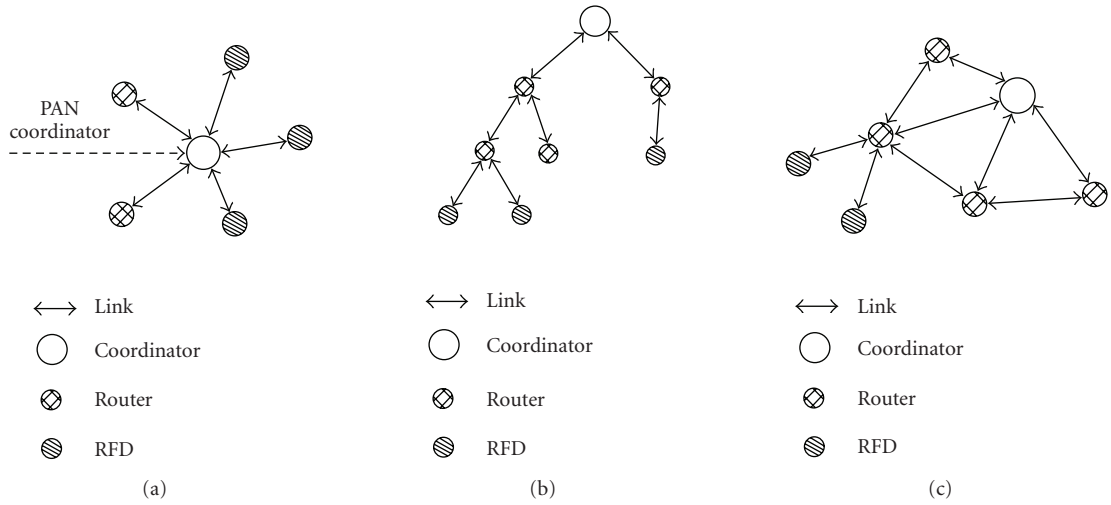

Figure 1: Possible typologies for a Zigbee network: (a) *star*, (b) *cluster-tree*, and (c) *mesh*.

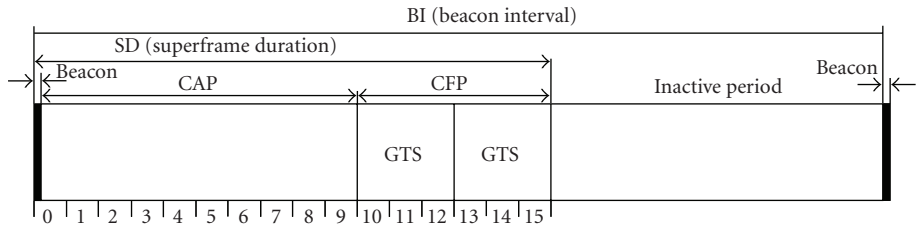

Figure 2: Frame structure of the *beacon* signal in a Zigbee network.

CSMA/CA MAC protocol [25], with the use of a proper *back-off* algorithm [21], as required by the IEEE 802.15.4 standard. In the *contention-free period* (CFP), instead, only nodes with a reserved time slot can try to transmit data packets, so that collisions can be avoided. In order to allow safe data transmission, a *guaranteed time slot* (GTS) may be reserved to nodes which require it [26, 27]. In this portion of time, only these nodes can transmit, finding, therefore, the channel free. The dimensions of the beacon frame and the durations of the active phase (also called *superframe duration*, SD) and the GTS are defined by two parameters which are exchanged within the beacon signal. This signal is periodically sent by the coordinator in order to synchronize all remote nodes in the network and signal the beginning of the beacon frame, as shown in Figure 2.

Another feature of the Zigbee standard is the *end device binding*, similar to an association between two logical units residing in different nodes. For example, this is the case for the connections between lights and switches in a room. Various types of links are possible: (i) *one-to-one*, (ii) *one-to-many*, and (iii) *many-to-many*. Through end device binding, communications can be simplified and accelerated. In order to transmit data, the two binded nodes communicate through a 2-byte address given by the coordinator, instead of using the 8-byte address of the MAC level. This leads to a reduction of (i) the overhead in packet transmission, (ii) the processing time and, consequently, (iii) the energy consumption. The end device binding scheme is shown in Figure 3.

2.2. Z-Wave networks

Z-Wave is a proprietary wireless communication protocol designed for home control by Zensys [15], with special attention to commercial and residential applications such as distance measurements, light control, anti-intrusion detection, and so forth. The Z-Wave technology allows to create a high-efficiency network at a very low cost, especially if compared with other technologies currently available. In fact, a single Z-Wave chip, the basic entity which allows data exchange, costs less than 4 USD [16].

The transmission bands used by Z-Wave devices are the 868 MHz band in Europe and the 908 MHz band in USA. The Z-Wave communication protocol is a low-bandwidth half-duplex protocol designed to guarantee reliable wireless communications in a low-cost control network. The main purpose of this protocol is to send short control messages in a reliable manner from a control unit to one or more nodes in the network. In fact, the protocol is not designed to transfer large amounts of data or streaming/time-critical data.

The Z-Wave communication protocol consists of four layers: (1) the *MAC layer* (based on the CSMA/CA protocol), which includes the PHY layer of the ISO/OSI stack

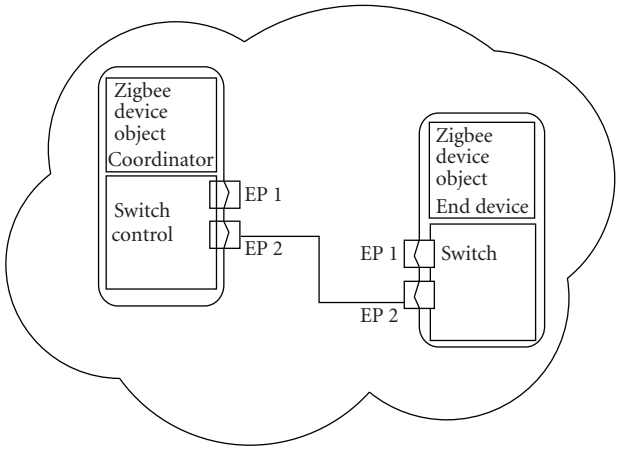

Figure 3: End device binding scheme of a Zigbee network.

and controls the radio frequency (RF) media; (2) the *transfer layer*, which controls the transmission and reception of frames; (3) the *routing layer*, which controls the routing of frames in the network; and (4) the *application layer*, which controls the payload in the transmitted and received frames [28]. The Z-Wave protocol includes two basic types of devices: *controllers* and *slaves*. Controlling devices are nodes that initiate control commands and send them out to other nodes, whereas slave nodes reply to these instructions and execute the required operations. Slave nodes can also forward the commands to other nodes, allowing the controller to communicate with nodes out of direct reach. The protocol employs a unique identifier number, referred to as home ID, to separate a network from another network nearby. A unique 32-bit identifier is preprogrammed on each controller node [29].

The Z-Wave communication protocol allows a maximum number of hops in the network. Because of the protocol design, it has to handle communications in a home environment, and consequently, it does not need to communicate data over long distances. The communication range in a free line-of-sight scenario is about 70 m, but it can fall down to $15 \div 20$ m in an indoor environment. However, Z-Wave nodes belonging to the series 100 and series 200 allow a maximum of four hops, so that the overall communication distance which can be covered in an indoor scenario is about 100 m.

The controller has the function of a master in the network. A Z-Wave network has always a mesh topology, and the maximum number of nodes which can be included is 232. The Z-Wave protocol is a low-rate (9.6 kbps) communication protocol. In the base module ZW0201 (Series 200), nodes that allow RF communications at 40 kbps have been introduced to reduce the latency period. The adopted solution guarantees compatibility, in the same network and without adaptors, between nodes that support 9.6 kbps communication and nodes that support 40 kbps communication. Moreover, no variation at the application layer is required.

A typical application of the Z-Wave protocol is the creation of a home control network, which consists of a complex set of nodes: battery-powered, DC-powered, fixed, and mobile. All these types of nodes need to be handled in different manners and are supported by the Z-Wave protocol. In particular, special attention is devoted to reduce the energy consumption and there are four different statuses for a battery-powered node: *sleep, normal* (no RF activity), *transmit*, and *receive*, with energy consumptions equal to 2.5 μA, 5 mA, 39 mA (at maximum transmission power), and 21 mA, respectively.

3. EXPERIMENTAL SETUP

3.1. Zigbee networks

In order to create an experimental setup for a Zigbee network, we consider PICDEM Z nodes belonging to the Microchip family. The PICDEM Z demonstration board is shown in Figure 4. This board has an embedded temperature sensor (referred to as TC77) and a radio frequency interface (referred to as Chipcon CC2420 chip). All nodes are completely reprogrammable through a programmer called MPLAB ICD 2. The Zigbee protocol stack is implemented through a code developed by Microchip, compiled through the MPLAB software packet, and downloaded on the node through the ICD 2 programmer. In fact, Zigbee is an open protocol and, in order to create a wireless sensor network based on the Zigbee standard, one has only to implement the desired version of the standard, adhering to the imposed constraints. The transmission range allowed by the PICDEM Z nodes is around 100 m in outdoor scenarios and 20 m in indoor scenarios. Each experimental trial considered for this work is repeated 500 times, in order to eliminate possible statistical fluctuations due to the instability inherent to the internal oscillator of the RF interface and possible measurement errors due to reflection and multipath phenomena. All the experiments are conducted in an indoor environment, so that there are reflections due to walls and furniture. The possible network topologies employed in our tests are shown in Figure 5. For every test, the number of nodes employed in the network and their roles are indicated. In particular, cases without routers (Figures 5(a) and 5(d)) and with intermediate routers (Figures 5(b) and 5(c)) are considered. All the experiments are performed using the 2.4 GHz band, since the actual version of the stack supports only this frequency band. The distances between the nodes in the considered experiments are a few meters, so that the attenuation phenomena can be neglected in the delay measurements. In addition, all the experiments have been performed in a beacon-disabled mode, because the current version of the Zigbee stack provided by Microchip does not support the use of beacon in operative conditions.

We point out that we were not able to obtain any experimental result considering the network topology in Figure 5(c). In fact, in all the considered network topologies of this type, we have observed processing problems: the first router manages almost always to connect directly to the coordinator before the second router could rely the received packets. This will be described in more detail at the and of Section 4.1.3, with particular reference to the results presented in Figure 11.

Figure 4: PICDEM Z demonstration board.

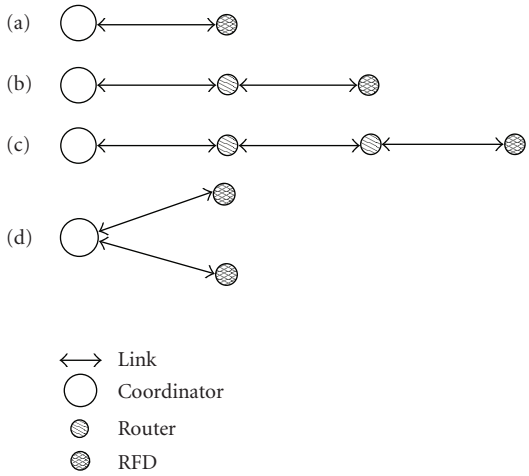

Figure 5: Network topologies employed for the measurements in Zigbee networks. Four possible scenarios are considered: (a) direct transmission between RFD and coordinator, transmissions through (b) one router or (c) two routers, and (d) transmission from two RFDs to the coordinator.

3.2. Z-Wave networks

The nodes employed in our Z-Wave experimental setup belong to the ZW0201 family: an illustrative node is shown in Figure 6. As previously mentioned, the use of the Z-Wave technology leads to the creation of mesh networks. The network scenario used in our experiments is shown in Figure 7: one controller (*tester*) and three slaves, referred to as *devices under test* (DUTs), are placed inside our department rooms. As shown in Figure 7, the *tester* node is placed in a room and DUTs are placed in different rooms. The direct distances between *tester* and DUTs are about 10 m and $21 \div 22$ m, respectively, for DUT 1 and for DUTs 2 and 3. Two network topologies are implemented in our tests, as shown in Figure 8: (a) the three slaves talk directly to the coordinator, or (b) two slaves talk to the coordinator through a router. The measurements carried out with a Z-Wave network are obtained by averaging over 10 000 experimental trials. The measurements are carried out in terms of *network connectivity*, which will be characterized as a proper function of the PER.

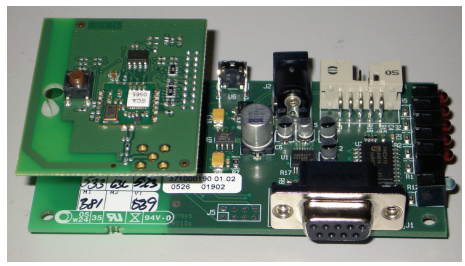

Figure 6: Z-Wave node with interface module.

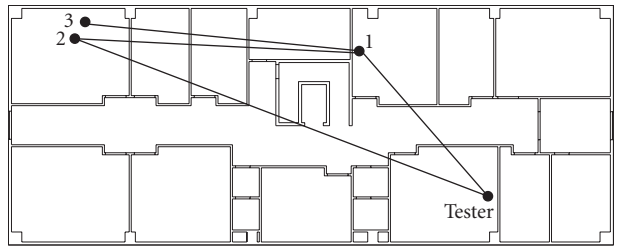

Figure 7: Experimental set up for Z-Wave network. The position of sensors (both tester and slaves) inside our department are pictured.

4. EXPERIMENTAL MEASUREMENTS

4.1. Zigbee networks

4.1.1. RSSI measurements

In the first set of experiments, the RSSI value detected by a node is stored. In particular, the impact of the distance between the two employed nodes is evaluated. The RSSI is a very important indicator for wireless networks, since it can be used to characterize the channel status. According to the CSMA/CA protocol, the node measures the received signal intensity, and if this intensity is higher than a fixed threshold, it waits for the end of the ongoing transmissions. In addition, the RSSI value has a key role also during the network creation phase. In fact, when the first node sets up the network, it must sense the channel to be used, in order to avoid the busy ones.[2] The other nodes, instead, must sense the channel to determine which channel the first node is transmitting in, so that a correct association process can start.

In order to obtain experimental measurements, the topology in Figure 5(a) has been considered, using two nodes directly connected: a coordinator and an RFD. The RFD, after the joining phase with the coordinator, starts transmitting. At the same time, the coordinator receives data packets and sends back an acknowledgment (ACK). At the network layer of the ISO/OSI stack (namely, layer 3) there is a parameter, denoted as RSSI, originating from the power detection per-

[2] When a coordinator sets up a new network, it starts sensing all the channels in order to find the first channel free and avoid other already created wireless networks.

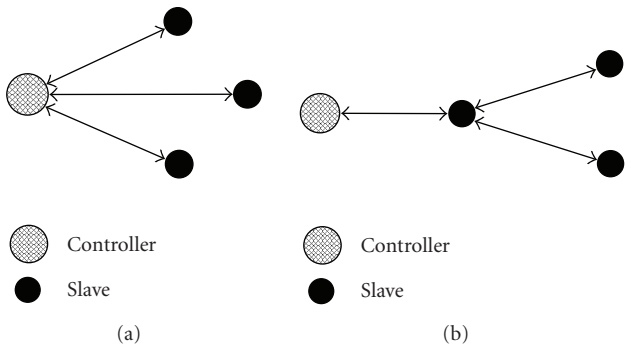

FIGURE 8: Network topologies for experimental measurements with a Z-Wave network. Two cases are considered: (a) direct transmission between slaves and controller, and (b) where one slave acts as an intermediate router.

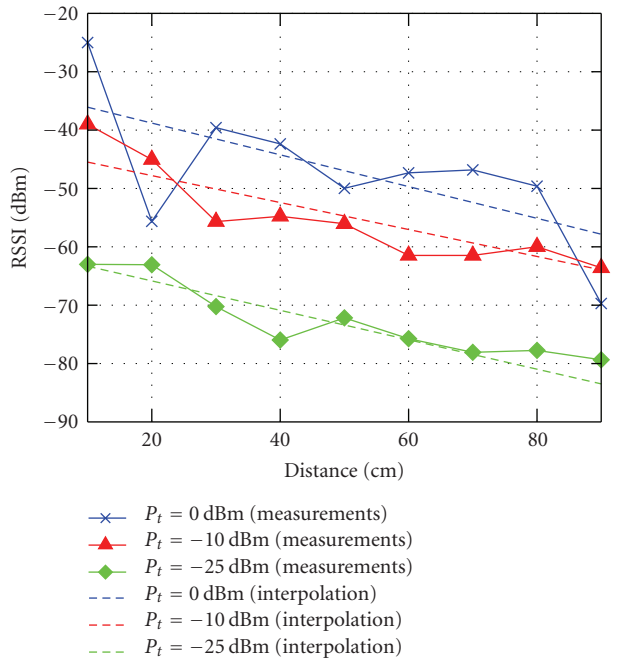

FIGURE 9: RSSI as a function of the distance between nodes. Three different values of the transmitted power are considered: (i) P_t = 0 dBm, (ii) $P_t = -10$ dBm and (iii) $P_t = -25$ dBm.

formed by the CC2420 at the physical layer, used to perform the actions discussed above. The physical layer, in fact, is responsible for all the tasks related to power management and medium access. The radio interface embedded on the PIC-DEM Z board (CC2420) mounts a *directional antenna*, and several antenna configurations can be considered. In this paper, we consider a 180-degree orientation between the two interfaces.

In Figure 9, the measured RSSI is shown as a function of the distance between the two nodes. Solid lines represent the effective values measured by the coordinator, whereas the dashed lines are obtained by linearly interpolating the collected experimental values. Three different values for the transmit power P_t are considered: (i) 0 dBm, (ii) −10 dBm, and (iii) −25 dBm. The difference between experimental values and dashed lines can be associated with the presence of reflection phenomena (due to walls and furniture) and obstruction phenomena (due to people crossing the rooms). In logarithmic scale, the RSSI decreases linearly, as expected, as a function of the distance. Obviously, increasing the transmit power leads to a better performance, since the environmental conditions are the same for all the measurements.

4.1.2. Throughput measurements with a point-to-point link

The goal of this experiment is to measure the throughput as a function of the number of nodes in the network and the packet length. We consider the topology shown in Figure 5(a), that is, a network where an RFD is transmitting directly to a coordinator. Various measurements are carried out, in correspondence to different values of the packet length. According to the Zigbee standard, the maximum possible packet length is 128 bytes at the MAC layer of the ISO/OSI stack. In order to avoid problems with the communication protocol, we use a lower value (e.g., 90 bytes). In fact, the Zigbee standard does not provide any fragmentation function for the packets. The throughput in this case is shown, as a function of the packet length, in Figure 10 (solid line). The throughput is calculated, over 50 received packets, as the ratio between number of bits received correctly and the total transmission time. This experimental procedure is repeated ten times.[3] The results in Figure 10 show that the throughput increases *less than linearly* as a function of the packet length. The goal of the standard is to guarantee a transmission data rate of 250 kpbs, but our tests show that a practical network performance is still far from this performance level. In fact, only a throughput of 32 kpbs can be achieved in the presence of the maximum offered traffic load.

4.1.3. Throughput measurements in the presence of routers

We consider the topologies where the packets transmitted from the RFD to the coordinator are relayed by one router (see Figure 5(b)) or two routers (see Figure 5(c)). The throughput measurements in these scenarios are shown, as solid and dashed lines, respectively, in Figure 10. The presence of a router influences heavily the data rate. In fact, according to the CSMA/CA protocol, a node can send data only if it finds the channel free. In the presence of a single RFD (as considered in Section 4.1.2), since the coordinator does not send data except for the ACK message to the RFD, the channel is always free for a transmission. In the configuration in Figure 5(b), instead, when the router retransmits its packets to the coordinator the medium is busy, so that the RFD must wait in order to transmit new data. In the presence of two hops, the throughput with the CSMA/CA protocol is reduced by a factor of two (because one of the nodes of a link is,

[3] Our experiments show that a Zigbee wireless network is very sensitive to channel impairments (reflections, etc.). In fact, communication errors appear very often, especially at the beginning of the transmission.

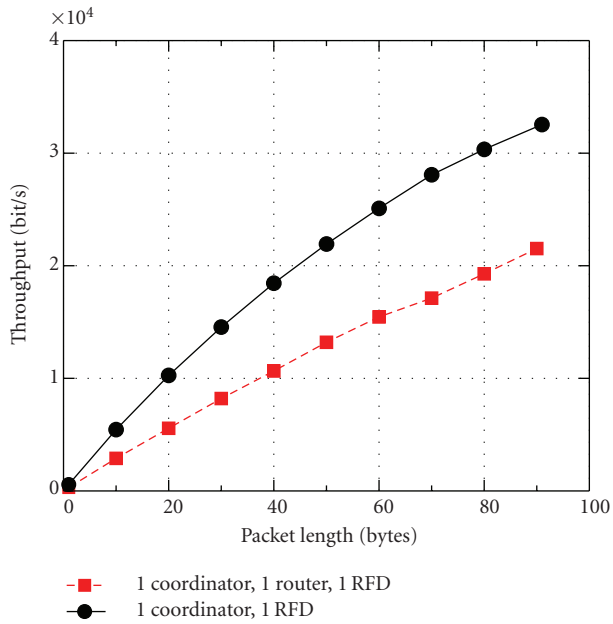

FIGURE 10: Throughput measurements results for the Zigbee network configurations shown in Figure 5(a) (circles) and Figure 5(b) (squares), respectively.

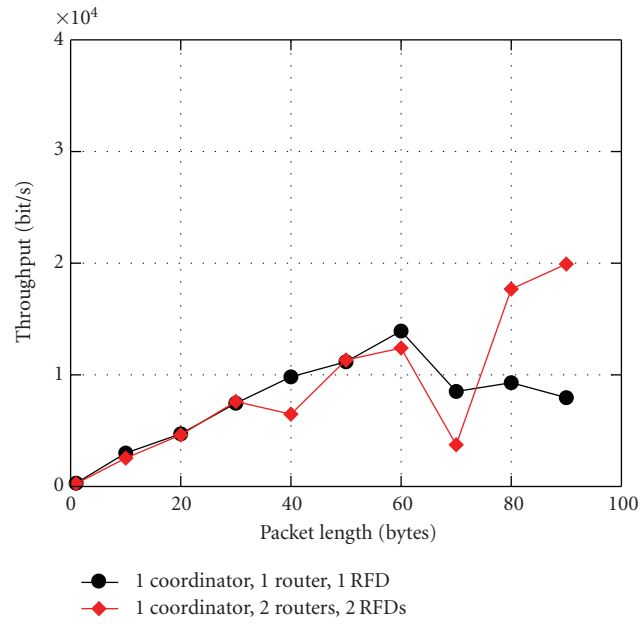

FIGURE 11: Throughput measurements results for the Zigbee network configurations shown in Figure 5(b) (circles) and Figure 5(c) (diamonds), respectively. The presence of interference due to people is taken into account.

alternatively, silenced). In general terms, the throughput decreases as $O(1/n_{\text{hops}})$, where n_{hops} is the number of hops traversed by a packet to reach its destination. As a matter of fact, the practical throughput is lower than that expected from the theoretical analysis, because of control messages exchanged by the nodes in order to notify the network of their presence.

In order to evaluate the impact of the environmental interference, we repeat the measurements carried out for Figure 10, the only difference being the presence of a much larger number of people moving across the sensor network laid in our department. The obtained results are shown in Figure 11. From these results, it is immediate to realize how deleterious the presence of walking people is. This is due to the fact that people introduce more reflection and fading effects, which are detrimental for the communication quality. It is therefore very important to reduce these effects, in order for wireless sensors to be used for home control applications. In addition, the router itself is not very stable. If some control messages are not correctly delivered, the router stops working, instead of recovering from the occurred errors and going on with its tasks. This is probably due to the "young age" of the standard, which was first proposed only in 2004.

The second topology of interest for throughput evaluation contains two routers, which relay the packets towards the destination (topology (c) in Figure 5). In this case, according to the theoretical analysis, the network throughput should be smaller by a factor of three with respect to that in the ideal case (topology (a) in Figure 5). However, the obtained experimental results are very similar to those relative to a topology with only one router, that is, the results shown in Figure 10. The Zigbee protocol, as explained in Section 2.1, implements the AODV routing protocol. This means that the nodes, which are not placed far from each other, tend to route the packets through a path with the lowest possible number of hops. In other words, the first router communicates directly to the coordinator, rather than making an intermediate hop with the second router.

4.1.4. *Throughput in the presence of two RFDs*

The last experimental test consists in measuring the network throughput in the presence of two RFDs which transmit simultaneously to the coordinator. This is the network topology shown in Figure 5(d). Unlike the scenario with one router and one RFD (i.e., the topology in Figure 5(b)), in this case there are two remote nodes transmitting directly to the coordinator which, in turn, has to send back the ACK to the correct node. Moreover, in a network with a topology as in Figure 5(b), the coordinator has to send back an ACK only if the message from the router is directed to the coordinator itself. In the scenario shown in Figure 5(b), the coordinator has to send back an ACK whenever it receives a message. Therefore, the number of collisions increases and a throughput reduction is expected. Since the nodes send data at the highest possible rate, when a node takes control of the channel, it tends to keep it for a long time. In fact, as soon as a node stops its transmission, it generates a new packet and tries immediately to send it: it is very likely that the channel will still be free, because it has just been released by the node itself. Analyzing the data collected from the measurements, the number of transmitted packets which reach the destination is unbalanced in favor of one of the two RFDs, confirming our

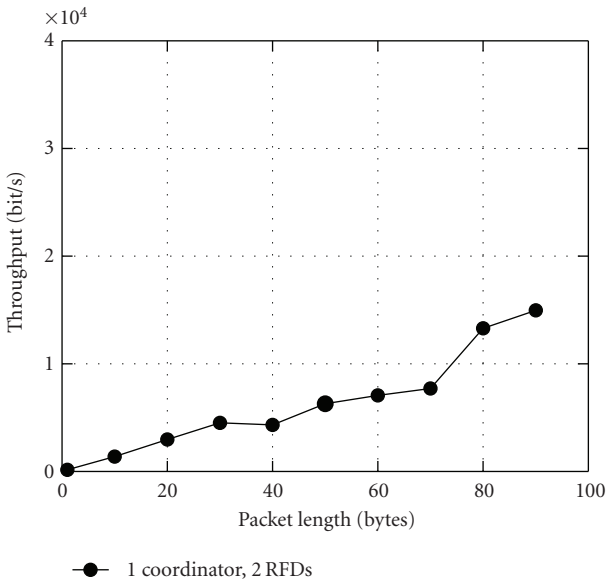

Figure 12: Throughput measurements for the Zigbee network configuration shown in Figure 5(b), that is, with two RFDs talking directly to the coordinator.

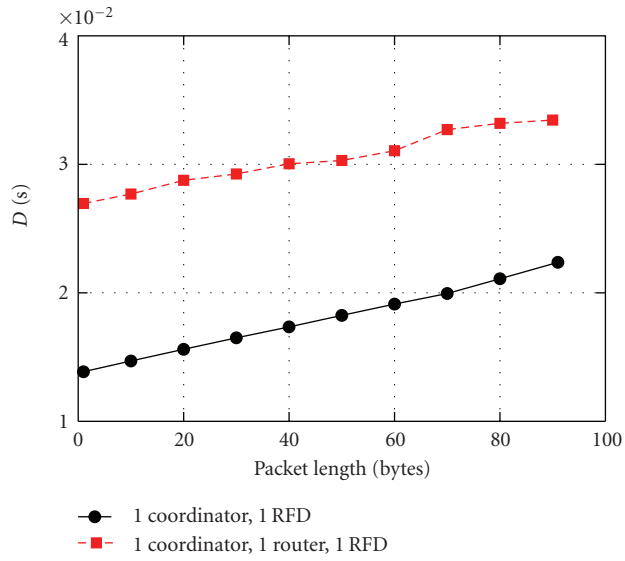

Figure 13: Delay measurement with direct transmission (scenario in Figure 5(a)) and 1-hop transmission (scenario in Figure 5(b)) in a Zigbee network.

intuition. In Figure 12, the throughput results are obtained by averaging over the throughputs of each RFD, considering 500 experimental trials. In this scenario as well, the experimental measurements are influenced by occasional events, like people crossing a link during a transmission.

These results have been obtained in a scenario where two RFDs are in the same carrier-sensing range. Otherwise, in fact, the *hidden terminal* problem (no RTS/CTS mechanism is provided by the Zigbee standard) occurs. In order to make a fair comparison, the packet generation rate must be sufficiently low for the number of collisions to be negligible. In fact, for high packet generation rate a node, which sends a packet, is likely to reutilize the channel at its subsequent attempt. The other node, in fact, due to the delay introduced by the backoff algorithm, may not be able to transmit at all or, at most, transmits only a few packets. If the packet generation rate is reduced, instead, the probability that one transmitting node finds the channel available increases. Therefore, data transmission can be considered balanced.

4.1.5. Delay performance in a Zigbee network

Another important indicator of network performance is the average delay between two consecutive packets correctly received by the coordinator. Consider now a scenario like that in Figure 5(a), that is, with direct transmission between an RFD and a coordinator. From a theoretical viewpoint, the transmission delay D_{direct} can be written as

$$D_{\text{direct}} = \frac{L}{R_b} + T_{\text{prop}} + T_{\text{proc}}, \tag{1}$$

where T_{prop} is the propagation delay, T_{proc} is the processing time at the node, L is the packet length, and R_b is the transmission data rate. The time T_{proc} includes both the processing delay introduced by the node and the delay introduced by the backoff algorithm. Since the average distance between nodes is around 3 m, the propagation delay is $T_{\text{prop}} \simeq 10$ nanoseconds, and therefore, can be neglected. Finally, one obtains

$$D_{\text{direct}} \simeq \frac{L}{R_b} + T_{\text{proc}}. \tag{2}$$

In Figure 13, the experimental results, in the cases with direct transmission from a remote sensor to the coordinator (solid line) and indirect transmission through a router (dashed line), are shown. Since in the case with a router there is a retransmission, the average delay almost doubles. Extending expression (2), the delay can be approximated as

$$D_{\text{router}} \simeq 2\left(\frac{L}{R_b} + T_{\text{proc}}\right) \tag{3}$$

since retransmission of the packet to the coordinator (including a double processing time) has to be considered. Note that expression (3) for D_{router} should also take into account the delay introduced by retransmission of packets after a transmission error, but we neglect this term because the nodes are placed close to each other—the distance between nodes is around 3 m. Therefore, as will be more clearly shown in Figure 16, at this distance the packet error rate is almost 0, then there is no increase of the total delay due to lost packets. A low interference scenario has been considered. This assumption is also motivated from the results in [30].

In Figure 14, the delay is shown as a function of the packet length, in terms of experimental, simulation, and theoretical results. The square symbols in Figure 14 are associated with the point-to-point experimental measurements

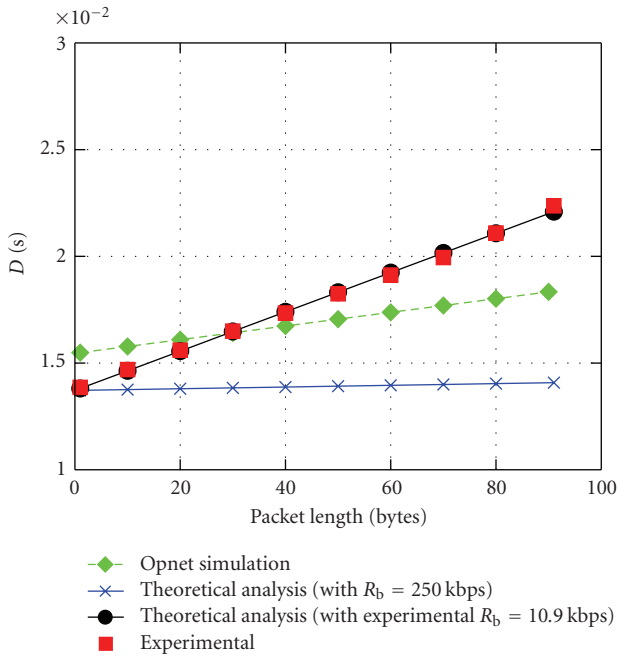

FIGURE 14: Delay analysis in a Zigbee network. Experimental, theoretical, and simulation results are shown.

described in Section 4.1.2. Then, we apply a first-order polynomial interpolation of these values, in order to derive the theoretical curve of delay (2) (curve with circular symbols). In addition, the curves associated with the maximum transmission rate provided by the standard (line with crosses) and with the estimated processing time of the node (line with circles) are also shown. The last curve (dashed line) in Figure 14 is obtained through the use of Opnet network simulator [18]—more details on the Opnet simulator will be given in Section 5. In order to make the comparison between simulations and experiments meaningful, the average delay calculated in the experiments is used as the packet interarrival time for the simulations. Therefore, with small packet lengths, the obtained delay is quite large (in fact, the real packet interarrival time is rather short). On the other hand, with larger packet sizes, the simulated delay is lower than the experimental delay. Note that the Opnet simulation curve shown in Figure 14 is obtained by adding to the exact simulation output an offset equal to the experimental processing time. The measured offset is equal to 13.7 milliseconds. This value can be interpreted as the processing time of the node, which includes data processing and input/output operations on serial registers.

4.1.6. *Packet error rate*

The PER corresponds to the ratio between the number of erroneous received packets and the total number of transmitted packets. However, the Zigbee communication protocol is equipped with an error control mechanism, to reduce the loss of data. This mechanism is based on the use of *automatic repeat request* (ARQ) techniques. More precisely, the Zigbee protocol requires up to three packet retransmissions in the absence of an ACK from the destination node. This technique guarantees a correct data delivery.

The first experiment is about the measurement of the PER, as a function of the distance, in a short communication range. Considering distances between 10 cm and 1 m, in order to make a comparison with the experiments described in Section 4.1.1, it turns out that the performance of the system remains practically unchanged. The experimental setup is basically the same, except for the precision of the measurements, obtained by averaging over 5000 transmissions.[4] The average PER is around 0.165. This high PER value is mainly due to synchronization problems of the nodes and internal exchange of messages at the control level of nodes. This confirms that the first version of the stack developed by Microchip suffers of "youth" problems.

The same experiment is repeated placing the two nodes in different rooms of the department, as shown in Figure 15. The results of our PER measurements at the coordinator, shown in the same picture, highlight the impact of attenuation (due to the walls) and reflections (due to the furniture) on the network performance. RFD 2 is a few meters closer to the coordinator than RFD 3, but it has worse PER performance than the other node, because its signal has to cross a larger number of walls to reach the coordinator. Besides, the presence of a metallic cabinet on the transmission path of RFD 2 degrades the overall performance. Even if RFD 2 and RFD 3 are a few meters behind RFD 1 (with respect to the coordinator), the performance falls down quickly, because of the limitations introduced by the indoor environment.

In order to overcome the aforementioned problems of stability, a new version of the stack has been developed by Microchip. The current experimental setup consists of three RFDs placed in the same room, sending messages to the coordinator at the highest possible rate, avoiding the sleep period introduced by the beacon frame. The coordinator replies to these messages with an ACK, in order to confirm correct packet delivery. In these conditions, the results of our experiment show that it is possible to perform data transmission with a PER equal to $10^{-2} \div 10^{-3}$. This feature makes a Zigbee network suitable for applications with *quality of service* (QoS) not too stringent requirements, like transmission of uncoded voice signals.

The results of the last performance analysis of a Zigbee network, in terms of PER, is shown in Figure 16, where the "connectivity indicator," defined as 1-PER, is shown as a function of the distance between the two transmitting nodes. The network topology adopted in this experiment corresponds to that in Figure 5(a). According to the Zigbee protocol, two communication strategies, in the presence of message delivery errors, are considered: (i) 4 retransmissions (solid line) and (ii) no retransmission (dashed line with diamonds).

[4] In order to obtain accurate measurements, at low PERs, the number of trials should be larger, but the chosen value is a compromise between precision of analysis and total duration of the test.

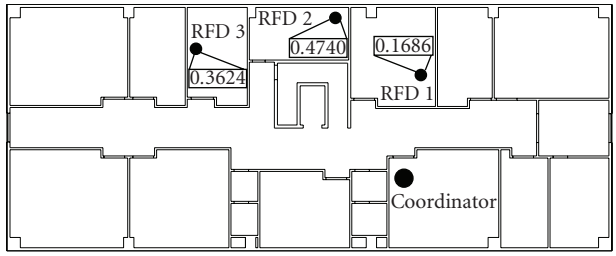

Figure 15: Scenario for packet error rate measurements.

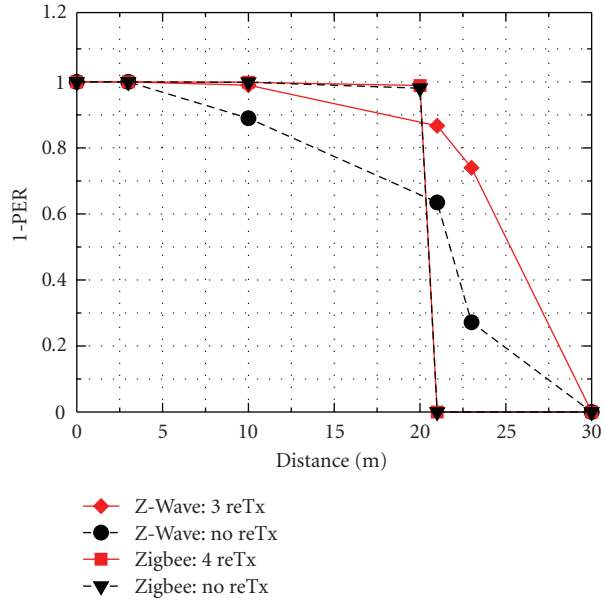

Figure 16: Connectivity, as a function of the distance, in an indoor environment for a Zigbee and Z-Wave networks. Two cases are considered for the Zigbee standard: (i) absence of retransmissions (dashed line with triangles) and (ii) four retransmissions (solid line with squares). Two scenarios are considered also for the Z-Wave standard: (i) absence of retransmissions (dashed line with circles) and (ii) three retransmissions (solid line with diamonds).

According to theoretical results, an ad hoc wireless network has a bimodal behavior [17, 31, 32]. At short distances, there is full connectivity and communication can be sustained. When the distance between the two nodes increases beyond a threshold value, instead, connectivity falls down rapidly and the two nodes can no longer communicate. Looking at Figure 16, it can be observed that there is no difference between the performance in the presence or absence of retransmissions. This means that if there is connectivity between nodes in a Zigbee network, then packet delivery to destination is guaranteed *regardless* of the number of retransmissions. Finally, one should observe that the critical maximum distance for connectivity in indoor environment is around 20 m. This value is radically different from that expected from the Zigbee standard in an open-space scenario, corresponding to approximately 100 m. The connectivity indicator (1-PER) in Figure 16 has a sharp bimodal behavior. We believe that this is due to strong multipath phenomena in our indoor scenario. In fact, our measurement environment differs substantially from typical (outdoor) simulation assumptions [33].

4.2. Z-Wave networks

4.2.1. Packet error rate

The communication system can be characterized in terms of connectivity or, equivalently, PER. The connectivity has been calculated for three different scenarios, depending on the presence of routing in the communication and the packet retransmission mechanism to recover from transmission errors. The transmission power has been set to 0 dBm for all the cases. The three considered scenarios are

(1) the scenario in Figure 8(a), with no routing and no retransmission;
(2) the scenario in Figure 8(a), with retransmission and no routing;
(3) the scenario in Figure 8(b), with retransmission and routing.

The retransmission mechanism works as follows: if a packet is lost or is not acknowledged by the slave, the controller retransmits the same packet twice, waiting an interval, between consecutive retransmissions, given by a backoff counter (as described in the CSMA/CA protocol [25]). If packet transmission fails after the retransmissions, the packet is declared lost. The experimental setup is shown in Figure 7. The tester node (controller) sends test packets to the other nodes (slaves), which reply with an ACK packet. If the ACK arrives correctly to the controller, the transmission is considered successful and the tester sends the next packet, increasing the counter associated with the transmitted packet. Otherwise, the tester waits a backoff time and retransmits the packet. Two possible network topologies, shown in Figure 8, are considered: in the first one there is a direct link from the tester to the DUTs, whereas in the second one node 1 acts as a router to connect nodes 2 and 3.

The results of these tests are shown in Table 1. The difference between node 2 and node 3 resides only on the type of the antennas, but the results obtained are not very different in the two considered cases (the maximum deviation is around $5 \div 10\%$). As for Zigbee networks, in this case as well it has been observed that the interference generated by people passing in front of a node or placing themselves in front of the tester might break the connection.

In order to better describe the connectivity behavior of a Z-Wave network, the connectivity indicator, that is, 1-PER, is shown, as a function of the distance, in Figure 16. In particular, the presence or absence of retransmission mechanisms is considered. These curves are obtained by averaging over 1000 repetitions of the experiment. In these conditions, attenuation due to walls and doors, reflections due to metallic furniture, and link breakage due to people passing through or stopping in correspondence to the direct radio

Table 1: PER results in a Z-Wave network.

Scenario	Distance (m)	PER
1	10	1.1×10^{-1}
	21	3.65×10^{-1}
	23	7.28×10^{-1}
2	10	9.8×10^{-3}
	21	1.33×10^{-1}
	23	2.6×10^{-1}
3	10	7×10^{-3}
	21	4.3×10^{-2}
	23	5×10^{-2}

link increase considerably the variance of the measurements. However, the Z-Wave communication protocol guarantees good connectivity in a 1-hop link in an indoor (laboratory) environment, for a distance longer than 20 m.

4.2.2. Delay

The second set of measurements carried out with a Z-Wave network is relative to the delay. The delay per packet is calculated as the average (over the measurements) time interval between the beginning of a transmission of a packet and the beginning of the transmission of the following packet. This time is normally necessary for transmitting the packet, receiving the ACK (from all slaves connected to the tester), and processing the packet at the controller and the slaves. At high network traffic loads, or at low signal-to-noise ratios at the receivers, this delay is strongly affected by collisions (lost packets), and the consequent retransmissions by the controller. Referring to the three scenarios described at the beginning of Section 4.2.1 and recalled in Table 1, the measured delays can be summarized as follows:

(1) 39 milliseconds, when the transmitted value is fixed (fixed value);
40 milliseconds, when the transmitted value is variable (variable value);
(2) 43 milliseconds, with fixed value;
43 milliseconds, with variable value;
(3) 61 milliseconds, with fixed value;
86 milliseconds, with variable value.

More precisely, *fixed value* indicates that the transmitted value is always the same and there is no need to write it every time into the flash memory, whereas *variable value* indicates that the transmitted value needs to be written into the flash memory every time, with a consequent loss of time for the transmissions. These measurements are obtained by averaging over 1000 repetitions of the same experiment. One can see that writing into the flash memory has no relevance in a network scenario with low traffic load. In fact, with a higher load (due to routing and retransmissions), that is, in the third case in Section 4.2.1 and above, node 1 has to manage all packets in the network and writing into the flash memory leads to a loss of time and busy waiting for the packets. Therefore, the delay when the transmitted value is variable increases.

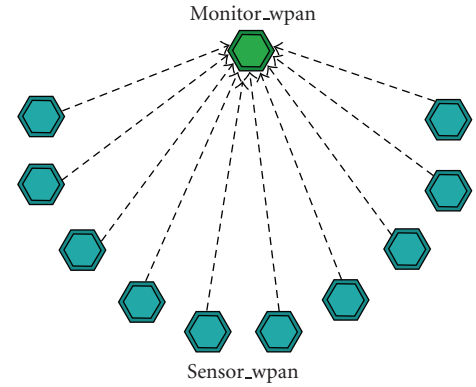

Figure 17: Opnet scenario for performance evaluation of Zigbee networks. An example with 10 RFDs (*Sensor_wpan* nodes) and 1 coordinator (*Monitor_wpan* node) is pictured.

5. SIMULATION RESULTS

In order to verify the experimental results obtained in Section 4, we also present simulation results of Zigbee networks using the commercial simulator Opnet Modeler 11.5 [18] and a built-in Opnet model provided by the National Institute of Standards and Technology (NIST) [34]. We note that only simulations for Zigbee networks are carried out, since Z-Wave is a proprietary protocol and the protocol stack is known only at the application level. The Zigbee model provided by the NIST implements only the first two levels of the ISO/OSI stack—that is, the levels corresponding to the IEEE 802.15.4 standard—and only a few functions of the upper layer. Therefore, the major part of the control messages required by the Zigbee standard is not transmitted in the considered network simulation model.

In Figure 17, the Opnet scenario used for performance evaluation of Zigbee networks is shown. In particular, an example with 10 RFDs (referred to as "Sensor_wpan") and 1 coordinator (referred to as "Monitor_wpan") is pictured. The task of the monitor is to receive packets and, then, compute the average transmission delay between two consecutively received packets. In this case, the delay corresponds to the difference between the last backup instant and the reception instant. The RFD, instead, sends data packets with a data rate $R_b = 250$ kbps and a constant generation interval $g = 0.02$ second. All packets have fixed length equal to 720 bits/pck. All nodes in the network implement the protocol stack described in Section 2.1. In particular, the channel access with the CSMA/CA protocol is *unslotted*, that is, the GTSs are not used in the SD. Moreover, the following backoff algorithm is implemented when a collision is verified.

(i) The node tries to send its packet when the actual transmission ends.[5]

[5] Note that the CSMA/CA algorithm uses a *1-persistent* strategy [21].

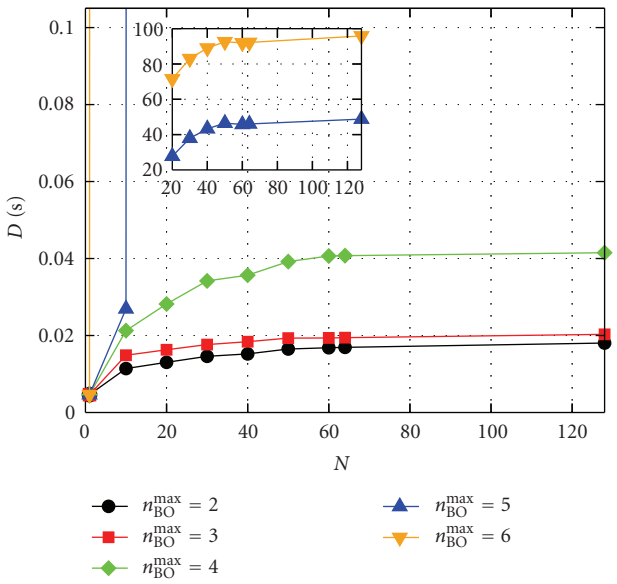

FIGURE 18: Simulation values of delay in a Zigbee network varying the maximum backoff. The box contains a zoom of the curves associated with $n_{BO}^{max} = 5$ and $n_{BO}^{max} = 6$ at high values of the delay.

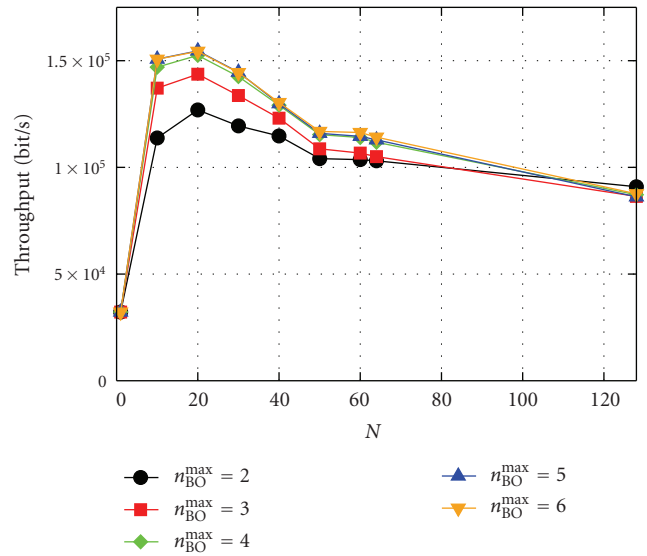

FIGURE 19: Simulation values of throughput in a Zigbee network varying the maximum backoff.

(ii) If a new collision happens, the node tries to transmit again after a time

$$T_1 = \alpha T_{pck}, \tag{4}$$

where α is randomly chosen in the interval $[0, 2^{B-1})$, $T_{pck} = L/R_b$, and B is a suitable integer constant.

(iii) When a new collision happens, the new backoff time is given by

$$T_j = 2T_{j-1}, \quad j = 2, \ldots, n_{BO}^{max}, \tag{5}$$

where n_{BO}^{max} is the maximum backoff number chosen by the user.

(iv) From the n_{BO}^{max}th iteration on, the backoff time remains fixed to

$$T_{max} = 2^{n_{BO}^{max}-1} T_{pck}. \tag{6}$$

The simulation results are collected as a function of the number of nodes in the network, varying the maximum backoff counter number n_{BO}^{max}. In Figure 18, the delay is shown, as a function of the number of nodes, for various values of the maximum backoff number n_{BO}^{max}. If n_{BO}^{max} is small, the delay remains low, regardless of the number of nodes. When a high value of n_{BO}^{max} is used, the delay increases abruptly for increasing number of nodes. This is due to the higher traffic load offered to the network. While, in the first case, the retransmission occurs quickly, in the second case the node has to wait for a longer time before attempting to retransmit. All the curves shown in the figure have a floor. This value depends only on the maximum backoff number n_{BO}^{max} in the network. The delay value for larger number of nodes is, in fact, dominated by the maximum backoff value, given by (6). Note that inside Figure 18, another small figure is inserted. This figure represents a "zoom" of the two curves associated with $n_{BO}^{max} = 5$ and $n_{BO}^{max} = 6$ at high values of the delay, in correspondence to which they saturate. The choice of inserting a zoomed figure inside Figure 18 is an expedient to show that the delay saturates for any value of n_{BO}^{max}. However, one can observe that increasing n_{BO}^{max} from 4 to 5 causes an explosion of the delay. In fact, $n_{BO}^{max} = 4$ is the maximum backoff value adopted in the standard [6], probably because it had already been verified that higher values of n_{BO}^{max} make the system unstable.

In Figure 19, the throughput at the coordinator is shown, as a function of the number of transmitting nodes, for various values of the maximum backoff counter number n_{BO}^{max} (as in Figure 18). All simulation results are obtained using a packet length of 720 bits and a packet interarrival time of $g = 0.02$ second. Since a larger number of transmitting nodes correspond to a higher traffic load offered to the network, we obtain the typical throughput curve of a network which employs the CSMA/CA protocol [21]. In addition, we can observe that if the maximum backoff counter becomes higher, the throughput at the monitor increases. This can be easily explained considering (6). If we use a small backoff value, all the nodes which sense a collision try to retransmit after a short interval, and consequently, the collision probability is high. With a higher backoff value, instead, the retransmission interval is longer, and therefore, the total number of successful transmissions increases.

Our last simulation results, shown in Figure 20, are associated with a throughput-delay analysis. The same setup of the previous experiments is employed. The curves shown in Figure 20 are parameterized curves, obtained by combining the throughput curves in Figure 19 and the delay curves in Figure 18, through the parameter given by the number of transmitting nodes. The network behavior evidenced by

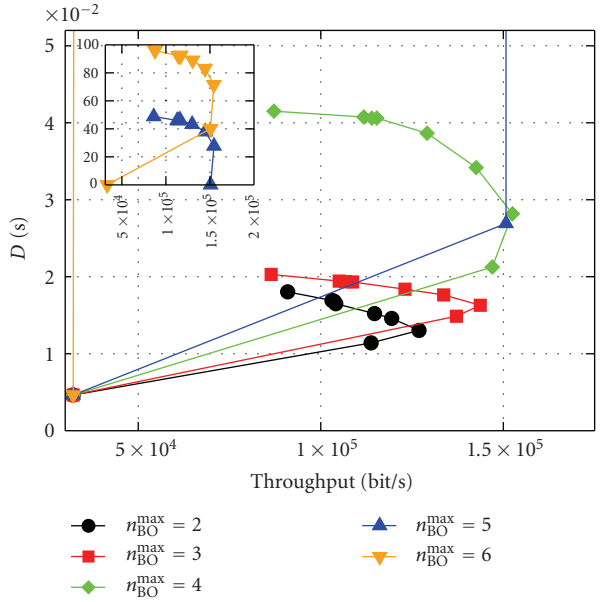

FIGURE 20: Simulation values of throughput-delay in a Zigbee network varying the maximum backoff. The box contains a zoom of the curve for high values of delay and throughput.

TABLE 2: Experimental and simulation results for a Zigbee network.

Results	D (s)	Throughput (bit/s)
Experimental	0.02237	21527
Simulation	0.004636	32186

the curves in Figure 20 is typical of a network adopting the CSMA/CA protocol. For a given maximum backoff counter, the corresponding curve presents an optimal working point, corresponding to a critical throughput. If one could use a dynamic backoff, one could guarantee, at the minimum possible delay, a maximum throughput approximately equal to 1.5×10^5 bit/s. The inner small box in Figure 20 has been included to show the throughput-delay behavior at high values of the delay—this is consistent with the results in Figure 18.

As previously mentioned, because of problems in the Zigbee stack developed by Microchip, we had not been able to perform an experimental analysis with more than 2 RFDs connected directly to the coordinator. Therefore, a direct comparison between simulation and experimental results is possible only for a scenario with 1 RFD. The results of this comparison are shown in Table 2. As one can see, the network performance predicted by the simulation is better than that observed in the experimental analysis. This is due to the absence of signal control in the Opnet model. In an experimental wireless sensor network, in fact, nodes have to exchange a lot of control messages (such as routing and application layer messages). In the Opnet scenario, instead, since only the first two levels of the ISO/OSI stack are implemented, none of these messages are sent, and therefore, the throughput is higher and the delay is lower.

6. CONCLUDING REMARKS

In this paper, we have considered two communication protocols for wireless sensor networks: Zigbee and Z-Wave. They have similar characteristics, but differ in some relevant aspects. In particular, since a Zigbee network is based on an open communication protocol, it is more "flexible" than a Z-Wave network, which, instead, is based on a proprietary protocol. The Zigbee communication protocol allows simpler interfacing between sensors, whereas the Z-Wave communication protocol, originally designed for control networks and not for monitoring, has more complicated connection features. We have analyzed the network performance using common indicators, such as *throughput*, *delay*, and *connectivity*. In particular, Zigbee networks have been studied using all performance indicators, and experimental measurements have been supported also by simulation results (using Opnet network simulator) and with the use of a simple analytical framework. The experimental results are in good agreement with simulation and analytical results. Z-Wave networks, instead, have been analyzed only in terms of connectivity experimental results (the Z-Wave protocol can be accessed only at the application level). A simulation or theoretical performance analysis of a Z-Wave network is, therefore, problematic. The obtained results, in terms of network connection, are similar for the two considered protocols. More precisely, in both cases the connectivity behavior is *bimodal*, that is, the connectivity is either full or basically inexistent.

REFERENCES

[1] I. F. Akyildiz and X. Wang, "A survey on wireless mesh networks," *IEEE Communications Magazine*, vol. 43, no. 9, pp. S23–S30, September 2005.

[2] R. Abileah and D. Lewis, "Monitoring high-seas fisheries with long-range passive acoustic sensors," in *Proceedings of MTS/IEEE 'Prospects for the 21st Century' Conference (OCEANS '96)*, vol. 1, pp. 378–382, Fort Lauderdale, Fla, USA, September 1996.

[3] S. Barberis, E. Gaiani, B. Melis, and G. Romano, "Performance evaluation in a large environment for the AWACS system," in *Proceedings of IEEE International Conference on Universal Personal Communications (ICUPC '98)*, vol. 1, pp. 721–725, Florence, Italy, October 1998.

[4] C.-Y. Chong and S. P. Kumar, "Sensor networks: evolution, opportunities, and challenges," *Proceedings of the IEEE*, vol. 91, no. 8, pp. 1247–1256, August 2003.

[5] S. N. Simic and S. Sastry, "Distributed environmental monitoring using random sensor networks," in *Proceedings of the 2nd International Workshop on Information Processing in Sensor Networks (IPSN '03)*, pp. 582–592, Palo Alto, Calif, USA, April 2003.

[6] "IEEE 802.15.4 Std: Wireless Medium Access Control (MAC) and Physical Layer (PHY) Specifications for Low-Rate Wireless Personal Area Networks (LR-WPANs)," *IEEE Computer Society Press*, pp. 1–679, October 2003.

[7] "IEEE 802.11 Std: Wireless LAN Medium Access Control (MAC) and Physical Layer (PHY) Specifications," *IEEE Computer Society Press*, pp. 1–459, June 1997.

[8] "IEEE 802.15.1 Std: Wireless Medium Access Control (MAC) and Physical Layer (PHY) Specifications for Wireless Personal

Area Networks (WPANs)," *IEEE Computer Society Press*, pp. 1–1169, June 2002.

[9] A. Sikora and V. Groza, "Coexistence of IEEE 802.15.4 with other systems in the 2.4 GHz-ISM-band," in *Proceedings of IEEE Instrumentation and Measurement Technology Conference (IMTC '05)*, vol. 3, pp. 1786–1791, Ottawa, Canada, May 2005.

[10] D. Cox, E. Jovanov, and A. Milenkovic, "Time synchronization for Zigbee networks," in *Proceedings of the 37th Annual Southeastern Symposium on System Theory (SSST '05)*, pp. 135–138, Tuskegee, Ala, USA, March 2005.

[11] O. Hyncica, P. Kacz, P. Fiedler, Z. Bradac, P. Kucera, and R. Vrba, "The Zigbee experience," in *Proceedings of the 2nd International Symposium on Communications, Control, and Signal Processing (ISCCSP '06)*, Marrakech, Morocco, March 2006.

[12] J.-S. Lee, "An experiment on performance study of IEEE 802.15.4 wireless networks," in *Proceedings of the 10th IEEE Conference on Emerging Technologies and Factory Automation (ETFA '05)*, vol. 2, pp. 451–458, Catania, Italy, September 2005.

[13] T. Sun, L.-J. Chen, C.-C. Han, G. Yang, and M. Gerla, "Measuring effective capacity of IEEE 802.15.4 beaconless mode," in *Proceedings of IEEE Wireless Communications and Networking Conference (WCNC '06)*, vol. 1, pp. 493–498, Las Vegas, Nev, USA, April 2006.

[14] Microchip, http://www.microchip.com/.

[15] Zensys, http://www.zen-sys.com/.

[16] "ZW0201 Z-Wave Single Chip," *Z-Wave technical documentation*, pp. 1–24, December 2005.

[17] O. K. Tonguz and G. Ferrari, *Ad Hoc Wireless Networks: A Communication-Theoretic Perspective*, John Wiley & Sons, Chichester, UK, 2006.

[18] Opnet, http://www.opnet.com/.

[19] A. Anandarajah, K. Moore, A. Terzis, and I. J. Wang, "Sensor networks for landslide detection," in *Proceedings of the 3rd International Conference on Embedded Networked Sensor Systems (SenSys '05)*, pp. 268–269, San Diego, Calif, USA, November 2005.

[20] Zigbee Alliance, http://www.zigbee.org/.

[21] A. S. Tanenbaum, *Computer Networks*, Prentice-Hall, Upper Saddle River, NJ, USA, 4th edition, 2003.

[22] C. E. Perkins and E. M. Royer, "Ad-hoc on-demand distance vector routing," in *Proceedings of the 2nd IEEE Workshop on Mobile Computing Systems and Applications (WMCSA '99)*, pp. 90–100, New Orleans, La, USA, February 1999.

[23] M. Neugebauer, J. Plönnigs, and K. Kabitzsch, "A new beacon order adaptation algorithm for IEEE 802.15.4 networks," in *Proceedings of the 2nd European Workshop on Wireless Sensor Networks (EWSN '05)*, pp. 302–311, Istanbul, Turkey, January-February 2005.

[24] Datasheet for CC2420 2.4 GHz IEEE 802.15.4/Zigbee Transceiver, http://www.chipcon.com/files/CC2420_Data_Sheet_1_3.pdf.

[25] L. Kleinrock and F. A. Tobagi, "Packet switching in radio channels: part I—carrier sense multiple-access modes and their throughput-delay characteristics," *IEEE Transactions on Communications*, vol. 23, no. 12, pp. 1400–1416, December 1975.

[26] J. Zheng and M. J. Lee, "Will IEEE 802.15.4 make ubiquitous networking a reality?: a discussion on a potential low power, low bit rate standard," *IEEE Communications Magazine*, vol. 42, no. 6, pp. 140–146, June 2004.

[27] E. Callaway, P. Gorday, L. Hester, et al., "Home networking with IEEE 802.15.4: a developing standard for low-rate wireless personal area networks," *IEEE Communications Magazine*, vol. 40, no. 8, pp. 70–77, August 2002.

[28] "Z-Wave ZW0102/ZW0201 Appl. Prg. Guide," *Z-Wave technical documentation*, pp. 1–242, December 2005.

[29] "ZW0102/ZW0201 Developer's Kit v4.10—Software Release Note," *Z-Wave technical documentation*, pp. 1–27, December 2005.

[30] N. Golmie, D. Cypher, and O. Rebala, "Performance evaluation of low rate WPANS for medical applications," in *Proceedings of IEEE Military Communications Conference (MILCOM '04)*, vol. 2, pp. 927–933, Monterey, Calif, USA, October-November 2004.

[31] R. Meester and R. Roy, *Continuum Percolation*, Cambridge University Press, Cambridge, UK, 1996.

[32] Y.-C. Cheng and T. G. Robertazzi, "Critical connectivity phenomena in multihop radio models," *IEEE Transactions on Communications*, vol. 37, no. 7, pp. 770–777, July 1989.

[33] D. Kotz, C. Newport, R. S. Grey, J. Liu, Y. Yuan, and C. Elliott, "Experimental evaluation of wireless simulation assumptions," Tech. Rep. TR2004-507, Dartmouth Computer Science Department, Hanover, NH, USA, 2004, http://www.cs.dartmouth.edu/reports/TR2004-507.pdf.

[34] National Institute of Standards and Technology (NIST), http://www.nist.gov/.